# Interface Interactions During Fabrication of Aluminum Alloy-Alumina Fiber Composites

C. G. LEVI, G. J. ABBASCHIAN, AND R. MEHRABIAN

The feasibility of fabricating fiber-reinforced aluminum alloys by addition of discontinuous fibers to vigorously agitated, partially solid metal slurries was investigated. In the first phase of the program, reported herein, emphasis was placed on the study of interface interactions between polycrystalline $Al_2O_3$ fibers and Al-2 to 8 pct Mg, Al-4.5 pct Cu and Al-4.5 pct Cu-1 to 2 pct Mg alloys. In general, it was observed that the incorporation of fibers could be readily achieved by this technique, and that fibers appeared wetted after a few minutes of contact with the melt. The composites produced exhibited an intimate, void free bond between the constituents. In addition, a region of significantly altered microstructure resulted from accumulation of oxide and/or aluminate particles which either formed within the melt and were attached to the moving fibers, or used the fiber surface as a substrate to grow on. Microscopic examination of this interaction zone and thermodynamic considerations indicate that it consists of fine $\alpha$-$Al_2O_3$, aluminates, oxides of the alloying elements, and probably some intermetallic compounds. For example, it is shown that a stable $MgAl_2O_4$ spinel forms at the interface of $Al_2O_3$ fibers and Al-Mg alloys. Examination of composite specimens fractured under tension indicated that the interfaces produced were strong enough to permit the transfer of loads at strengths in the order of 250 to 350 MPa.

## I. INTRODUCTION

THROUGHOUT their history, composites have evolved under the idea that a unique, tailored set of properties in a material can be obtained from a combination of constituents with (sometimes very) dissimilar characteristics. One of the main areas of interest has been the development of fiber-reinforced structural metals (*e.g.* Al, Ni, Ti), in which high strength fibers (*e.g.* $Al_2O_3$, graphite, SiC) or whiskers are coupled with a ductile matrix to produce a material that exhibits both properties. In these composites the prime function of the fibers is that of supporting most of the applied load, while the role of the matrix is to bind the fibers together and to transmit and distribute the external loads to the individual filaments. However, since the transfer of loads requires the existence of a bond and hence a certain degree of interaction between the constituents, the interface becomes a region whose nature and properties are critical to the performance of the composite structure.

Normally, it is desirable to have a strong enough interface which would permit transfer and distribution of load from the matrix to the filaments. Strong interfaces are typical of systems that are fully compatible, that is, the matrix and reinforcement form bonds but are mutually unreactive and insoluble. In the ideal case the perfect interface should be a mechanics continuum, involving coherency of the bond on the atomic level, and a chemical discontinuum, requiring the absence of any interdiffusion between the constituents.[1]

Interaction of the parent phases may be undesirable if it leads to the formation of weak interfaces, since premature failure at the matrix-fiber interface will limit the load carrying ability of the composite. Furthermore, when a finite interaction zone is produced, the properties of the material will decay after the reaction exceeds a critical level, and their final value will depend solely on the characteristics of the compound present at the fiber boundary.[2] Moreover, if the interaction produces an uneven or rough surface on the reinforcement, it may have a catastrophic effect on the fiber strength and therefore the composite properties.[3]

It is commonly agreed that alumina is an ideal reinforcing material for aluminum since the two are physically and chemically compatible at the projected service temperature of the resultant composites.[4] How-

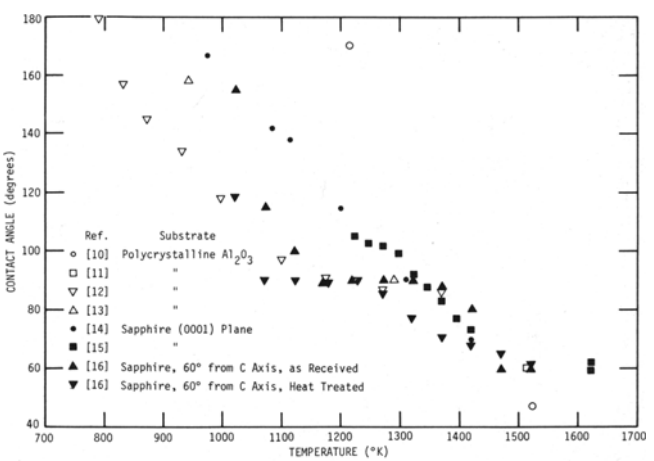


Fig. 1—Summary of reported contact angle data between aluminum and $Al_2O_3$ as a function of temperature.

C. G. LEVI is Graduate Student, Department of Metallurgy and Mining Engineering, University of Illinois, Urbana-Champaign, Illinois. G. J. ABBASCHIAN, Associate Professor, Department of Materials Science and Engineering, Pahlavi University, Shiraz, Iran, is presently Visiting Associate Professor, Department of Metallurgy and Mining Engineering, University of Illinois, Urbana-Champaign, Illinois, and R. MEHRABIAN is Associate Professor, Department of Metallurgy and Mining Engineering, Department of Mechanical and Industrial Engineering, University of Illinois, Urbana-Champaign, IL, 61801.

Manuscript submitted October 5, 1977.


ISSN 0360-2133/78/0510-0697$00.75/0

ever, the combination of these two constituents is complicated by the nonwetting characteristics of the system, and either coatings or alloying additions have to be used to promote interactions between the matrix and the filaments.

Interface interactions are then important not only in the performance of the composite but also in the design of appropriate fabrication techniques to produce the desired bond. This, in turn, involves the study of surface phenomena like wetting and chemical reactions, and their effect on interfacial bond strength.

Up to now, among the various processes attempted for the production of $Al_2O_3$-fiber reinforced aluminum, liquid infiltration has been the most successful.[5-9] An important limitation of this technique is the necessity for the liquid alloy to wet the fibers since for contact angles $\theta > 90$ deg the capillarity effects require the application of an external pressure to infiltrate the fiber bundles.[3] Unfortunately, the application of pressure alone does not solve the problem, since shrinkage occurring during solidification may be enough to cause debonding or void formation in the small channels between the fibers. Wetting is then desired from a fabrication viewpoint since it promotes maximum contact under equilibrium conditions.

A number of studies on the wetting behavior of the $Al/Al_2O_3$ system have been reported.[10-16] Results of these investigations for contact angle as a function of temperature are summarized in Fig. 1. These data, despite some inconsistencies, indicate that temperatures well above the melting point of aluminum would be necessary to induce a wetting condition ($\theta < 90$ deg). On the other hand, roughening and dissolution of $Al_2O_3$ substrates in contact with aluminum drops have been reported for contact angles larger than 90 deg.[14]

Other studies[11,14-16] have shown that contact angle instabilities at temperatures above 1400 K manifest themselves in spreading and contraction of aluminum sessile drops. Preferential attack of the $Al_2O_3$ substrate occurs at the liquid-solid-vapor interface leading to the formation of so-called "dissolution rings." Brennan and Pask[16] have explained this phenomena based on the formation of a $AlO \cdot Al_2O_3$ spinel-like structure on the $\alpha \cdot Al_2O_3$ surface, and its further reaction with aluminum to form the volatile species $Al_2O$.

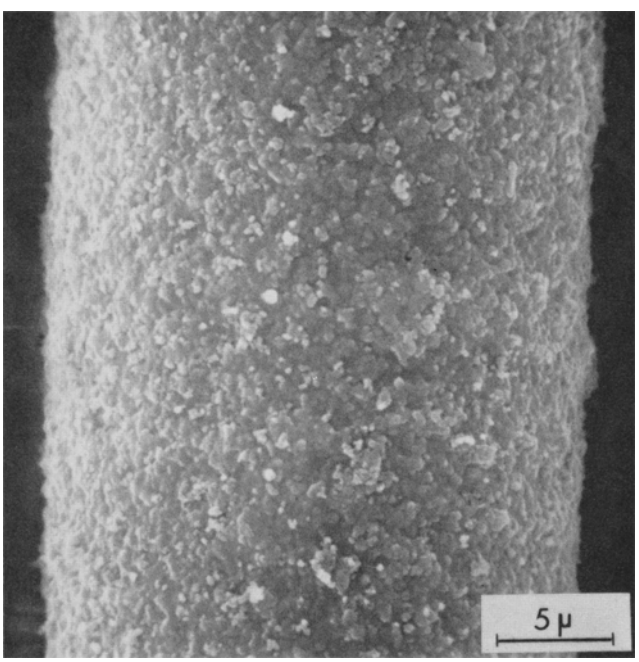


Fig. 2—SEM view of as-received $Al_2O_3$ FP fiber.

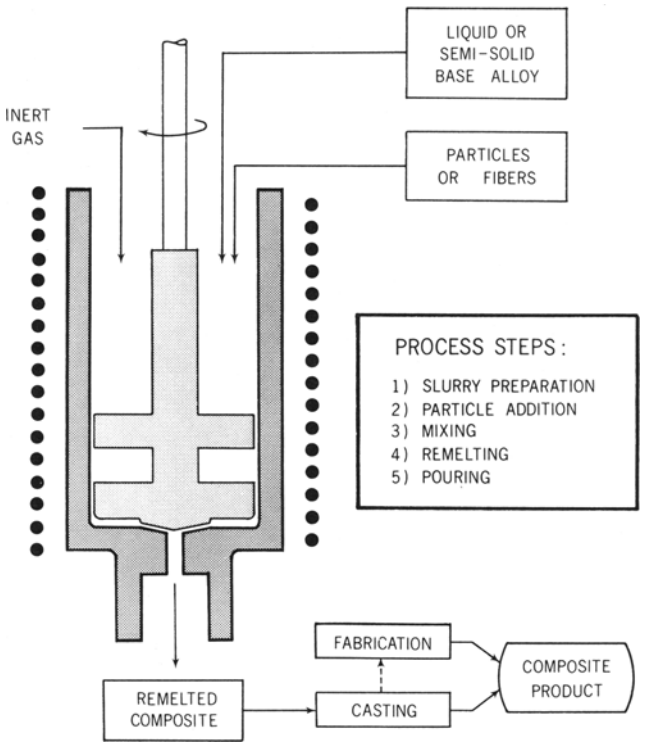


Fig. 3—Schematic of the apparatus for fabrication of aluminum matrix composites in the liquid-solid range.

Fabrication of $Al/Al_2O_3$ composites is then limited by the nonwetting characteristics of this system, and two different approaches to this problem have been investigated. The first one involves the use of sputtered coatings like Ni(Ti), Ni(Cr), and 1020 carbon steel[5,7] which physically attach to the fiber surface and are wetted by the liquid metal. However, most coatings readily dissolve in molten aluminum and may cause debonding unless the fabrication time is short, on the order of a few minutes. The second approach to enhance wetting calls for the use of alloying additions that can interact chemically with the ceramic material creating a desired new phase at the solid-liquid boundary.[8] Several authors have proposed that elements with greater affinity for oxygen (as measured by the free energy of oxide formation) than the solvent will preferentially concentrate at the interface,[17] reducing the surface energy ($\gamma_{SL}$) as described by the Gibbs adsorption equation. However, in the case of $Al/Al_2O_3$ all the alloying additions that have higher affinity for oxygen than the aluminum also tend to reduce $Al_2O_3$ and modify the chemical nature of its surface.

It is known that $Al_2O_3$ readily reacts with many divalent transition metal oxides to form aluminates which are isostructural with the mineral spinel of composition $MgAl_2O_4$. Several investigators[4,18,19] have indicated that spinels or similar oxides may be used to promote interfacial bonding since they have the potential to form strong bonds with both metals

and ceramics. If one accepts this point of view, then aluminum alloys containing Mg, Cu, Zn, or Fe become particularly interesting since they could form aluminate compounds under the appropriate conditions. Although some of these reactions have been observed with $Al_2O_3$ refractory bricks[20-22] only a few additions have been reported to promote sufficient wetting of uncoated $Al_2O_3$ fibers for successful liquid infiltration.[8,9] These additions normally involve the use of Li (which forms $Li_2O \cdot 5Al_2O_3$ at the interface) with the consequent problems of preparation and handling of the alloy, and the control of the chemical interaction during the fabrication process to avoid fiber degradation.

The work described herein is the first part of a multi-phase program, the overall aim of which is to study the feasibility of fabricating $Al_2O_3$ fiber reinforced aluminum alloy composites by incorporation of discontinuous filaments into a partially solidified, vigorously agitated metal slurry. The first phase of this program was mainly concerned with the study of the formation of bonds and related interfacial phenomena during the fabrication process. Two series of experiments were conducted for this purpose. In one series continuous fibers were immersed into static pools of fully liquid alloys, while in the other discontinuous fibers were incorporated into agitated baths of partially solid metal slurries. The latter approach was used to prepare composites containing from 1 to approximately 15 vol pct of fibers with a variety of alloys as matrices. The structure of the composites, and especially the interaction zone, were analyzed using different microscopy techniques. Some composites with more than 10 vol pct fiber were extruded and fractured under tension to examine the behavior of the matrix-reinforcement bond. Copper and magnesium were selected as alloy additions because both have been reported to reduce the contact angle between aluminum and $Al_2O_3$.[14]

## II. APPARATUS AND EXPERIMENTAL PROCEDURE

### 1. Materials

The alloys utilized in these experiments were prepared *in situ* from commercially pure aluminum (99.7 pct), magnesium (99.8 pct) and copper (99.95 pct).

**Table I. Summary of Composites Fabricated in the Liquid-Solid Range**

| Run | Matrix Alloy* | Fiber† Content (Vol. pct) | Addition Temp. (K) | Addition Time (min) | Total Residence Time‡ (min) |
|---|---|---|---|---|---|
| 1 | Al-4.5 pct Cu | 1 | 910 | 2 | 50 |
| 2 | Al-4.5 pct Cu-0.8 pct Mg | 2 | 900 | 60 | 75-135 |
| 3 | Al-8 pct Mg | 1 | 873 | 5 | 60 |
| 4 | Al-4 pct Mg | 1 | 903 | 5 | 90 |
| 5 | Al-2 pct Mg | 1 | 913 | 5 | 145 |
| 6 | Al-4.5 pct Cu-2 pct Mg | 1 | 890 | 3 | 90 |
| 7 | Al-2 pct Mg | 12 | 910 | 35 | 12-40 |
| 8 | Al-4.5 pct Cu-2 pct Mg | 14 | 900 | 28 | 20-55 |
| 9 | Al-4.5 pct Cu-2 pct Mg | 14 | 900 | 20 | 10-30 |

*Degassed with $N_2$ except in run 1-3. Compositions given in wt pct.
†Initial fiber length was 3 mm except for run 8 where 6 mm fibers were used.
‡Total time includes the remelting which took 15 to 20 min on the average.

The incorporated material was Dupont's Type I $Al_2O_3$ FP fiber in the form of 3 and 6 mm long chopped filaments. This fiber is a continuous, multifilament yarn consisting of essentially pure, polycrystalline $\alpha$-$Al_2O_3$. Its reported tensile strength and elastic modulus are 1.4 to 2.0 GPa and ~380 GPa, respectively, and its density and melting temperature are $3.95 \times 10^3$ Kg/m$^3$ and 2318 K, respectively.[8,9] The filaments have a uniform cross section along their lengths, although variations in diam (15 to 25 $\mu$m) are observed from fiber to fiber. SEM examination of the fibers showed a microscopically rough surface, Fig. 2, which was not altered by heating at high temperature (15 min at 1270 K). TEM analysis indicated that the fibers have a very fine grained structure (~0.5 $\mu$m average grain size) and almost no internal pores.

### 2. Experiments With Static Liquid Alloys

The apparatus used to study the interaction between continuous fibers and static liquid alloys consisted of two small resistance heated furnaces located in a closed chamber. The lower furnace was used to hold the molten metal (~100 cm$^3$) in an alumina crucible. The upper furnace was used to preheat the fibers (as individual filaments or bundles), which were stretched on a C-shaped alumina tube and firmly held in place with a ceramic air setting cement. This assembly was manipulated from outside the chamber in a manner that that permitted controlled immersion of the fibers into the constant temperature melts. Prior to each experiment the system was flushed with argon gas. The alloy was then melted and the fibers, previously preheated to ~1270 K, were immersed in the metal bath at predetermined rates. When the operation was completed, the metal was rapidly solidified; the resulting ingot was then taken out, sectioned according to the immersion sequence, and polished for micro examination.

### 3. Experiments With Semisolid Alloys

The experiments for fabrication of composite materials were conducted using alloys in the semisolid state. The process has been previously described[23] and is based on the utilization of a viscous metal slurry prepared by partial solidification concurrent with vigorous stirring.

A schematic illustration of the apparatus used is shown in Fig. 3. It consisted of a mullite-graphite crucible inside a resistance heated furnace with maximum operating temperature of ~1270 K, and a carbon double-blade stirrer driven by a variable speed DC motor. The whole assembly was built on a frame, which permitted the stirrer to be moved vertically and be positioned properly inside the crucible. The crucible had an opening at the bottom which was used to pour out the material after processing.

The as-received $Al_2O_3$ consisted of large lumps of tangled fibers, and could not be charged as such into the melt. The problem was solved by using a vibrating hopper with internal screens, which was situated above the crucible and discharged the separated fibers directly on top of the melt.

The experiments carried out in this part of the program are listed in Table I. For each one the charge

alloy of the desired composition was melted in an induction or resistance furnace under protective atmosphere. After degassing, the metal was poured into the compositing apparatus where it was stirred and slowly cooled under continuous flow of argon until its temperature reached the desired value in the liquid-solid range. When a slurry of approximately 0.5 volume fraction solid was obtained, the argon flow was stopped and the fibers were fed as rapidly as possible; addition times for each experiment are listed in Table I. Subsequently, the argon flow was resumed while the metal was reheated to above its liquidus temperature and cast through the bottom hole in preheated graphite molds.

Some of the resulting ingots containing randomly oriented fibers were hot extruded in order to align the filaments in a particular direction.

### 4. Microstructural Examination

The general features of the microstructure, *e.g.* fiber distribution, volume fraction and orientation, matrix grain structure, second phase distribution and fracture surfaces were studied using a metallograph and a Scanning Electron Microscope. In most cases the samples were polished with diamond compound on napless paper after grinding with 600 grit SiC paper in the normal fashion.

Samples at several stages in the process were qualitatively and semiquantitatively analyzed using microprobe X-ray methods. Element distribution maps, step and continuous scanning patterns through the fibers and their surroundings were obtained from this apparatus. Energy Dispersion Spectroscopy (EDS) and Back Scattered Electron Images (BSEI) were also used with some success to examine the structure of the interaction zone.

Microchemistry and Electron Diffraction Analysis were attempted on thin films of the composites, using a JSEM-200 microscope equipped for transmission and scanning-transmission work. Phase identification was complemented with X-ray diffractometry of powders obtained by chemical dissolution of the matrix and grinding of the residual fiber material.

## III. RESULTS AND DISCUSSION

### A. Processing

Attempts to incorporate the fibers into static liquid alloys (Al-4 pct Mg and 8 pct Mg) were unsuccessful. As shown in Fig. 4(*a*) the originally spaced fibers were pushed together into a bundle. In addition to this, the melt surface formed a nonwetting meniscus around the fibers. Furthermore, the multifilament yarn was not infiltrated by the alloys and only the fibers at its periphery came into partial contact with the liquid melt. These observations are consistent with the nonwetting conditions reported for several aluminum alloys near their liquidus temperatures (<980 K).[14] This phenomenon has been attributed to the presence of oxide films on the melt surface or adsorbed contaminants on the ceramic substrate. Nevertheless, it should be mentioned that the fibers located at the periphery of a bundle, which were forced to have at least partial contact with the melt, eventually de-

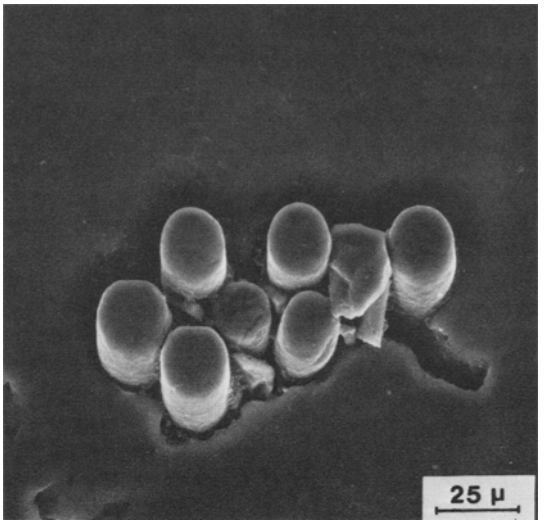


(*a*)

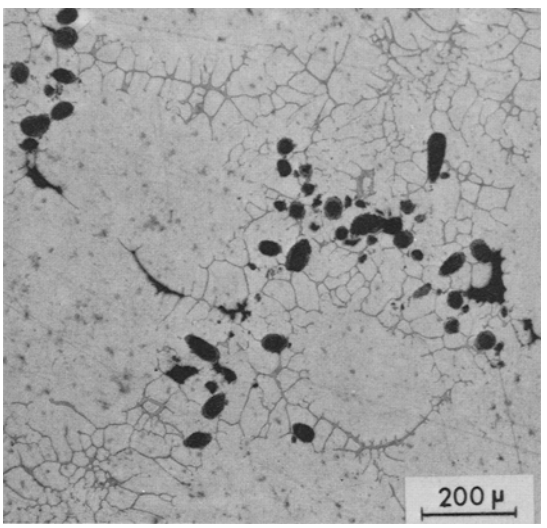


(*b*)

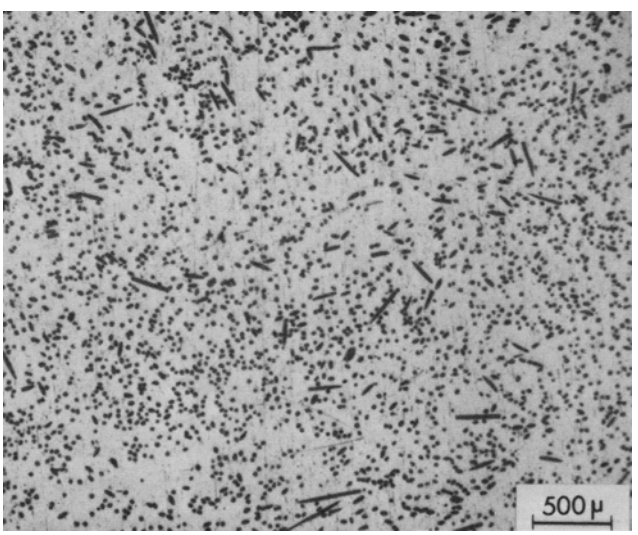


(*c*)

Fig. 4—(*a*) SEM view of $Al_2O_3$ fibers inserted into a completely liquid bath of Al-8 pct Mg alloy; the fibers originally spaced were pushed together without appreciable infiltration, (*b*) optical photomicrograph showing discontinuous fibers incorporated and dispersed in the originally liquid portion of the alloy slurry, (*c*) appearance of the cast composite subsequent to reheating above the liquidus temperature.

veloped some sort of interaction and appeared to be joined to the metal.

Addition of discontinuous fibers to an agitated bath of partially solid alloy proved to be much more effective in producing fairly homogeneous dispersions of $Al_2O_3$ fibers bonded to the matrix. To explain this result it is postulated that the fibers are kept submerged and dispersed by the agitation and the moving primary solid particles of the slurry, Fig. 4(*b*), until they develop an interaction and bond with the matrix. Rubbing from the metal particles should aid in disruption of contaminant films that hinder interaction, and expose "fresh" $Al_2O_3$ surface to the liquid. Furthermore, the fibers are expected to be brought into close contact with the melt due to the strong convection induced by the stirring. Suction samples taken from the bath indicate that after a relatively short time (<10 min) most of the fibers had interacted with the metal.

Metallographic examination of the as-cast ingots showed a fairly uniform distribution of randomly oriented fibers in the final composite, Fig. 4(*c*), leading to the conclusion that the interaction was enough to keep the fibers dispersed and wetted even after remelting of the solid particles in the slurry. Only slight agitation of the completely liquid melt was necessary to prevent settling of the incorporated material – due to differences in density – before the casting operation.

Among the present shortcomings of the process is the breakage of fibers into small segments ($l/d < 15$) that occurs during the incorporation as well as the extrusion step. Furthermore, it was observed that large reductions in area (>30 : 1) would be necessary to obtain an acceptable alignment via hot extrusion. A

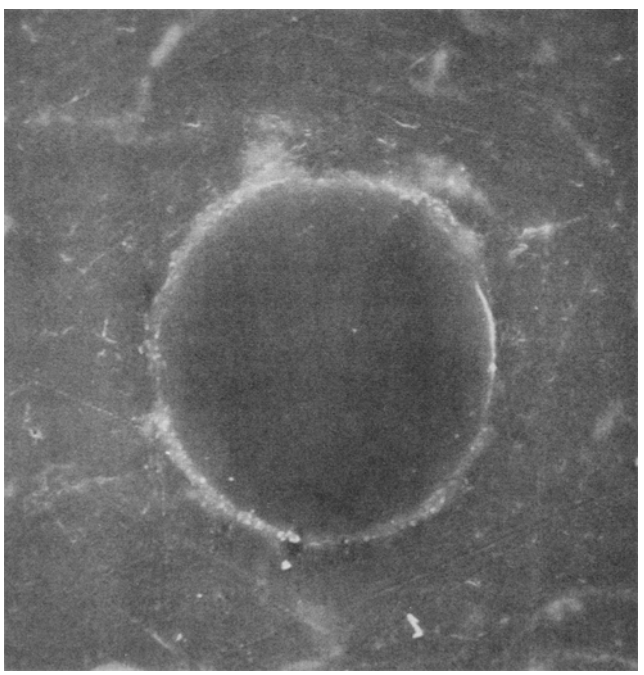


(*a*)

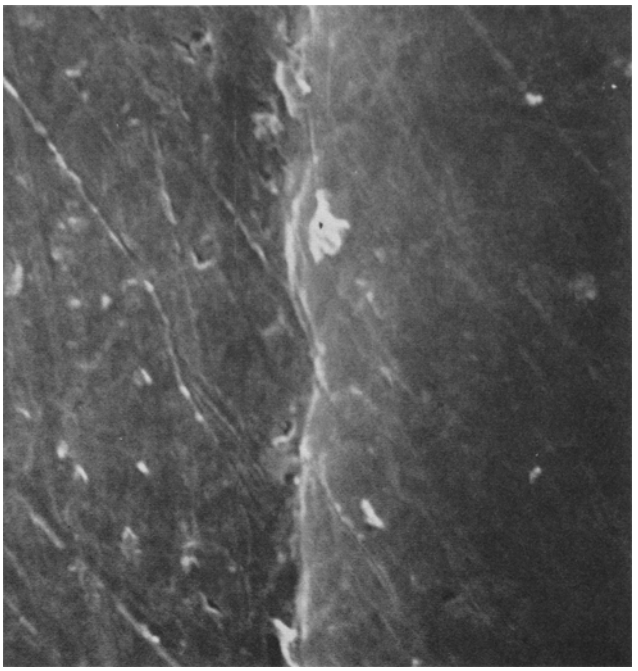


(*b*)

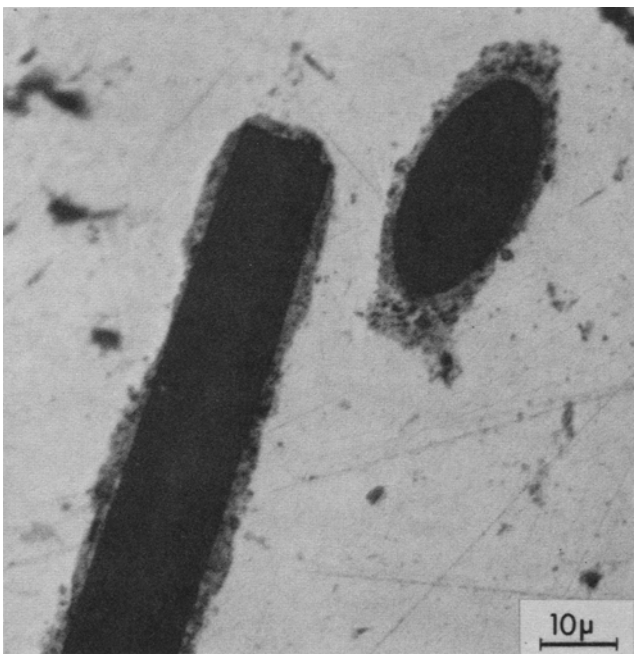


(*c*)

Fig. 5—Typical appearance of interaction zones. (*a*) SEM view of a fiber and its surroundings in an Al-4.5 pct Cu alloy, (*b*) SEM view of the fiber boundary in an Al-4.5 pct Cu alloy, (*c*) "apparent interaction zones" after long times in contact with an Al-4 pct Mg alloy slurry.

third problem associated with the apparatus is the entrapment of gas through the vortex formed by stirring, which causes oxidation and some porosity in the material produced. However, it is believed that the problems described above can be overcome by appropriate modifications of the system, such as changes in the geometry of the mixing chamber, utilization of longer fibers, working under vacuum and extrusion in the partially solid state. This phase of the investigation is presently underway and will be reported in a later paper.

## B. Interface Interactions

The major contribution of this work has been to show that $Al_2O_3$ fibers can be incorporated in aluminum alloy matrices that were previously thought to be inappropriate for composite fabrication. The nonwetting conditions that normally limit the application of liquid infiltration techniques were not a problem for fabrication in the liquid-solid range. Moreover, some degree of interaction between the fibers and the matrices occurred in all the alloys investigated. If interactions are thermodynamically possible, even at temperatures below the liquidus, then the difficulties for incorporation in the liquid state may be due to slow kinetics or physical barriers that prevent direct contact between the constituents. These barriers were somehow eliminated during fabrication by the present method and the kinetics was activated.

1. Appearance of the Interaction Zone. A common feature observed in all the composites fabricated is the existence of an intimate contact between the fibers and their surroundings, Fig. 5(*a*) and (*b*). Another characteristic usually found is the presence of a significantly altered microstructure around the fibers, which herein will be referred to as the "apparent interaction zone." This zone is readily identified by optical examination. It normally looks irregular in cross section and large variations in its thickness are common along the length of a given fiber as illustrated in Fig. 5(*c*).* A satisfactory explanation for this phenomenon is not yet available, but it could be attributed to several factors:

a) the interaction may start in localized areas and then spread laterally with simultaneous radial growth,

b) the kinetics of the reactions may be anisotropic, and

c) the grinding effect of the moving primary solid particles could induce severe localized erosion.

Whatever the cause, the fact is that fibers that were exposed to the same conditions show very large differences in thickness of the "apparent interaction zone." Nevertheless, the average maximum thickness in a specimen was found to depend on residence time and alloy composition as shown in Fig. 6. It should be noted that some fibers which did not show an appreciable interaction zone (at ~1000 times) were still bonded to the matrix, indicating that the surface reactions responsible for wetting are not necessarily those associated with the formation of the "apparent interaction zone."

2. Interactions Between $Al_2O_3$ Fibers and Al-Mg Alloys. Matrix alloys of 2, 4 and 8 pct magnesium were used to study the effect of this element on the interface interactions between aluminum and $Al_2O_3$. Since the experiments were done with alloys in the partically solid state, the liquid in which the fibers were incorporated and held was enriched in the alloying element. Liquid compositions of 4.3, 6.4, and 12.7 pct Mg corresponding to the nominal alloys 2, 4 and 8 pct Mg, respectively, were calculated from the equilibrium phase diagram and the process temperatures listed in Table I.

Typical "apparent interaction zones," for Al-Mg/$Al_2O_3$ composites consist of a mixture of discrete dark particles embedded in a lighter matrix, as shown in Fig. 5(*c*). Further examination of these zones indicated that:

a) the darker particles decrease in size and become fewer as the magnesium content in the alloy increases, and

b) the matrix in the interaction zone appears grayish in color in the lower magnesium content alloys and yellowish in the 8 pct Mg alloy.

Data for the average maximum thickness of the apparent interaction zone ($x$), Fig. 6, seem to fit a relationship of the type:

$$x = at^n$$

where $t$ is the residence time and $a$ and $n$ are positive constants. Calculated values of $n$ for the 2, 4 and 8 pct Mg were 0.57, 0.59 and 0.38, respectively. Since the irregular shape of the interaction zones makes it difficult to assign a unique value for the thickness in a particular sample, the data in Fig. 6 represent only general trends. Nevertheless, the relative positions and slopes of the lines in this figure, and the optical observations reported above, indicate the possibility of differences in the interaction mechanism and products between the lower magnesium content alloys and the 8 pct Mg alloy.

A common feature revealed by microprobe X-ray analysis was the existence of a Mg-enriched region around the fibers as illustrated in Fig. 7. Step scanning analysis across the fibers and their surroundings showed a distinctive magnesium peak at the fiber boundary. While significant variations of the relative intensity $I/Io$ (*i.e.*, normalized fraction of counts off standard) were noted around a given fiber, as well as

*The thick interaction zones shown in this and other micrographs were intentionally produced by holding the composites in the liquid-solid range for long times. Much smaller zones (~1 μm) were obtained with reduced agitation and shorter residence time during preparation of high fiber-volume-fraction composites.

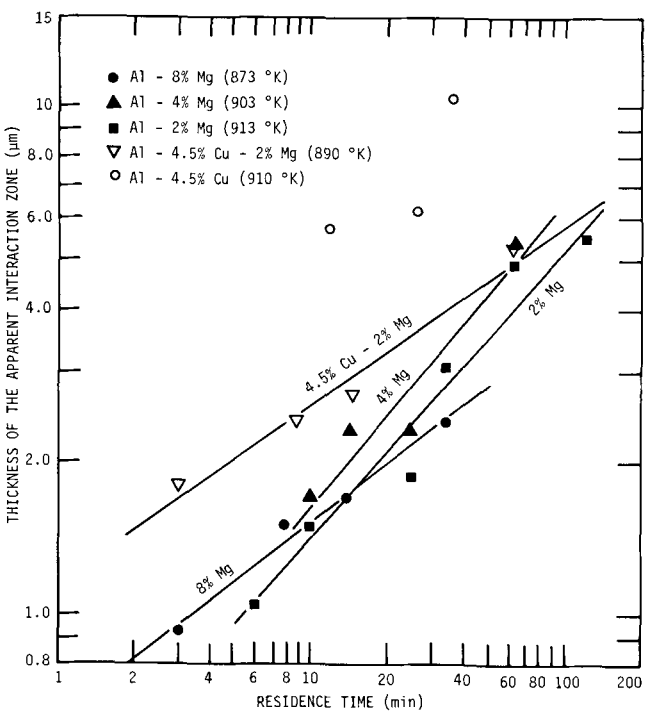


Fig. 6—Average maximum thickness of the "apparent interaction zone" as a function of residence time.

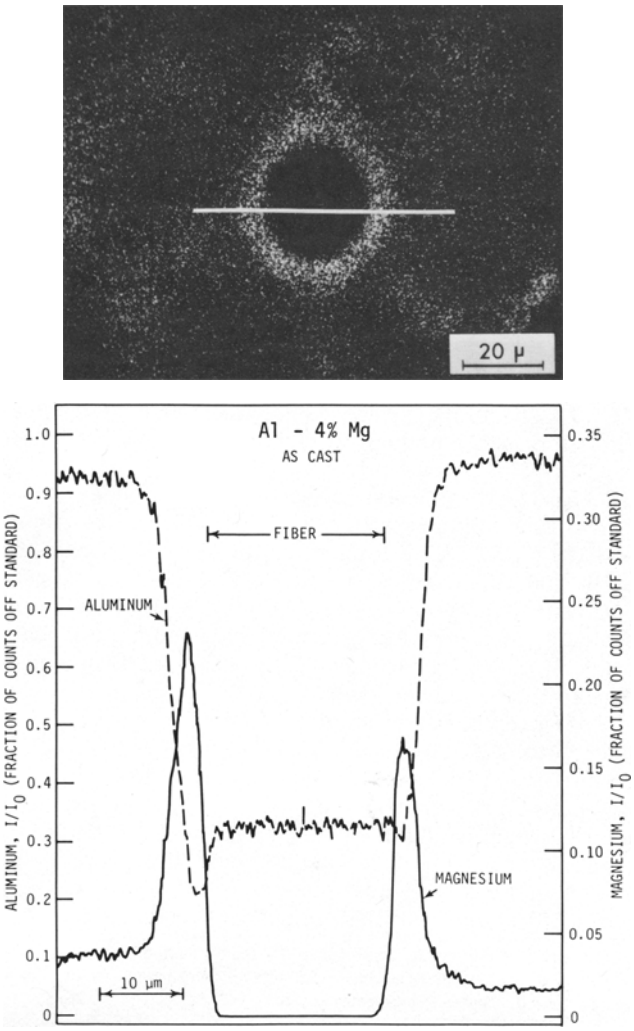


Fig. 7—Elemental Mg X-ray map and corresponding line scanning pattern for a fiber in an Al-3.8 pct Mg alloy. Note the Al depletion corresponding to the highest Mg peaks. The line on the map denotes the approximate scanning path.

from fiber to fiber, maximum $I/Io$ values for all the alloy compositions were consistently noted at the fiber boundary. In some cases these maxima were associated with a depletion of aluminum below that of the $Al_2O_3$ composition, Fig. 7. Furthermore, it was found that the Mg-rich zone around the fibers persisted after heat treatment (24 h at 685 K) in the aluminum solid solution region of the Al-Mg phase diagram, Fig. 8. This led to the conclusion that a stable reaction product was responsible for at least part of the magnesium accumulation at the fiber-matrix interface.

The "apparent interaction zones" were examined at progressively higher magnification via SEM and TEM. General observations from this work revealed that:

a) there is intimate contact between the fibers and the interaction zone,

b) the interaction zone is composed of material much finer in grain size than the neighboring fiber and matrix, and

c) large differences in magnesium composition exist between the parent phases and the interaction zone, as well as within the zone itself.

Energy Dispersion Spectroscopy (EDS) performed on several locations right next to the $Al_2O_3$ fiber surface gave an Al/Mg count ratio of approximately 2 : 1. This phenomenon was very localized at the fiber edge, and although magnesium was detected throughout the interaction zone, other locations in it produced smaller peaks.

Electron diffraction from areas in the vicinity of the fiber showed the presence of fine polycrystalline $\alpha$-$Al_2O_3$ in the interaction zone, and indicated that the material at the fiber edge (richest in magnesium) is probably $MgAl_2O_4$ spinel. This was further supported by X-ray diffractometry of fibers extracted from the composite after reaction.

Thermodynamic calculations, presented in Table II, show that the formation of $MgAl_2O_4$ at the processing

**Table II. Free Energy Changes for the Reactions of Interest***

| Reaction | Nominal Alloy Composition | | | | | |
|---|---|---|---|---|---|---|
| | 2 pct Mg | 4 pct Mg | 8 pct Mg | 4.5 pct Cu | 4.5 pct Cu 0.8 pct Mg | 4.5 pct Cu 2 pct Mg |
| $2[Al] + \frac{3}{2}(O_2) = <Al_2O_3>$ | −1388 | −1391 | −1401 | −1388 | −1391 | −1394 |
| $[Mg] + \frac{1}{2}(O_2) = <MgO>$ | −508 | −509 | −512 | | −467 | −478 |
| $[Cu] + \frac{1}{2}(O_2) = <CuO>$ | | | | −29 | −32 | −33 |
| $2[Cu] + \frac{1}{2}(O_2) = <Cu_2O>$ | | | | −13 | | |
| $<MgO> + <Al_2O_3> = <MgAl_2O_4>$ | −28 | −28 | −28 | | −28 | −28 |
| $[Mg] + \frac{4}{3}<Al_2O_3> = <MgAl_2O_4> + \frac{2}{3}[Al]$ | −39 | −43 | −52 | | −31 | −41 |
| $[Mg] + 2[Al] + 2(O_2) = <MgAl_2O_4>$ | −1888 | −1915 | −1962 | | −1886 | −1900 |
| $3[Mg] + <Al_2O_3> = 3<MgO> + 2[Al]$ | −33 | −46 | −73 | | | |
| $[Cu] + \frac{1}{2}(O_2) + <Al_2O_3> = <CuAl_2O_4>$ | | | | −30 | −32 | −33 |
| $[Cu] + 2[Al] + 2(O_2) = <CuAl_2O_4>$ | | | | −1467 | −1423 | −1427 |
| $[Cu] + [Al] + (O_2) = <CuAlO_2>$ | | | | −756 | | |
| $<CuAlO_2> + \frac{1}{2}<Al_2O_3> + \frac{1}{4}(O_2) = <CuAl_2O_4>$ | | | | −16 | | |

*$\Delta G_T$ in KJ/mole, calculated from data in Refs. 24–26.

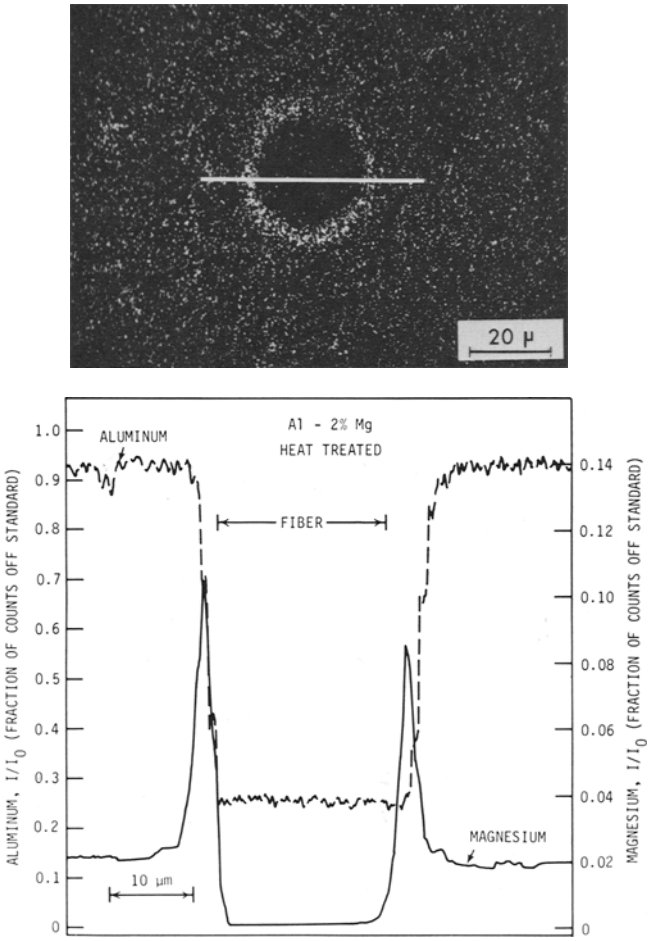


Fig. 8—Elemental Mg X-ray map and corresponding line scanning pattern for a fiber in an Al-2 pct Mg alloy after heat treatment (24 h at 685 K). The line on the map denotes the approximate scanning path.

temperatures is possible from any of the following reactions:*

*Symbols: <solid>, (gas), [in solution].

$$\langle MgO\rangle + \langle Al_2O_3\rangle = \langle MgAl_2O_4\rangle \quad [1]$$

$$[Mg] + 4/3\ \langle Al_2O_3\rangle = \langle MgAl_2O_4\rangle + 2/3\ [Al] \quad [2]$$

$$[Mg] + 2[Al] + 2(O_2) = \langle MgAl_2O_4\rangle. \quad [3]$$

Although spinel can form by reaction of $Al_2O_3$ and MgO—produced from direct oxidation of magnesium in the melt—this process is thought to be kinetically slow because it involves a solid state reaction. On the other hand, $MgAl_2O_4$ could form at the expense of $Al_2O_3$ in the fiber, following Reaction [2]. In this case the reaction product is expected to form a continuous layer on the fiber surface and grow by a diffusion mechanism. This would change the nature of the surface and may well be the phenomenon responsible for the initial wetting of the fibers. However, it is believed that the production of spinel from this source is somewhat limited, since the surface of the fibers did not appear heavily reacted or degradated, even after long residence times (~2 h). On the other hand, Reaction [2] could preferentially take place with the finer $Al_2O_3$ resulting from oxidation of the melt. This process requires the presence of oxygen and is equivalent to Reaction [3], which may occur within the melt, where the fibers could provide a suitable substrate for the growth of the aluminate. Availability of oxygen is not considered a limitation since the equilibrium partial pressure of oxygen ($p_{O_2}$) for Reaction [3] is of the order of $10^{-50}$. The vigorous agitation introduces enough gas bubbles to keep the $p_{O_2}$ inside the melt above this level. Whatever the mechanism, values of the standard free energies and activities at equilibrium indicate the existence of a large driving force for spinel formation, which increases with increasing magnesium content.

It should be mentioned that the occurrence of $MgAl_2O_4$ (17 pct Mg) is not sufficient to explain some of the measured high $I/Io$ values like that shown in Fig. 7. Therefore, it can be assumed that a significant amount of some compound richer in Mg, such as MgO (~61 pct Mg) or possibly nonequilibrium $\beta$-$Al_8Mg_5$ (36 pct Mg) is also present in the interaction zone.

The fine polycrystalline $Al_2O_3$ noted near the fiber boundary could have formed by direct oxidation of the melt, and clustered around the fibers in order to reduce the surface energy of the dispersion. This interaction seems very likely considering the high probability of collision between the different particles suspended in the stirred melt.

Thermodynamic calculations indicate that the formation of $Al_2O_3$, MgO and $MgAl_2O_4$ are likely to be competitive processes. However, in the low magnesium alloys, formation of $MgAl_2O_4$ is energetically more favorable. On the other hand, at some magnesium concentration between 4 and 8 pct (in the bulk alloy) the MgO becomes more stable than the $Al_2O_3$ as indicated by the equilibrium activity of magnesium*

*Values of equilibrium $a_{Mg}$ are 0.135 and 0.040 for nominal alloy compositions of 4 and 8 pct respectively. The calculated activities of magnesium in the enriched liquid were 0.018 and 0.050 respectively.

for the reaction

$$3[Mg] + \langle Al_2O_3\rangle = 3\langle MgO\rangle + 2[Al]. \quad [4]$$

These calculations could explain the changes in appearance of the interaction zone with alloy composition reported earlier in this section. The absence of the dark $Al_2O_3$ particles and the much favored formation of $MgAl_2O_4$ and MgO in the 8 pct Mg alloy would account for the observed difference in the appearance and thickness of the interaction zone.

3. Interactions Between $Al_2O_3$ Fibers and Al-Cu Alloys. An alloy containing 4.5 pct Cu was used to investigate interactions between $Al_2O_3$ fibers and the Al-Cu binary system. The calculated composition of the enriched liquid (for Experiment 1, Table I) corresponding to the process temperature of ~910 K was approximately 8 pct Cu.

As in the case of the Al-Mg alloys the "apparent interaction zone" is composed of a fine multiphase material, Fig. 9(*a*), and varies in cross section along the length of each fiber. However, the measured thickness of the zone was larger than that of the Al-Mg alloys at equivalent times, see Fig. 6, and a wider distribution in the data was noted.

A Back Scattered Electron Image of the fiber in Fig. 9(*a*) is shown in Fig. 9(*b*), where it is evident that the interaction zone contains a discrete Cu-rich "white phase" embedded in a continuous Cu-depleted gray phase. In addition, a large number of black particles,

presumably $Al_2O_3$, are also noted around the fibers of Fig. 9(*a*).

Differential etching techniques were used to determine the possibility of metallic phases occurring in the interaction zone. While the existence of $CuAl_2$ and small amounts of an iron rich phase, probably $Cu_2FeAl_7$, was established in the matrix of the composite, only minor amounts of both phases were noted in the interaction zone, but their size and shape were very different from the morphology of the "white phase" shown in Fig. 9(*b*). Furthermore, the bulk of the interaction

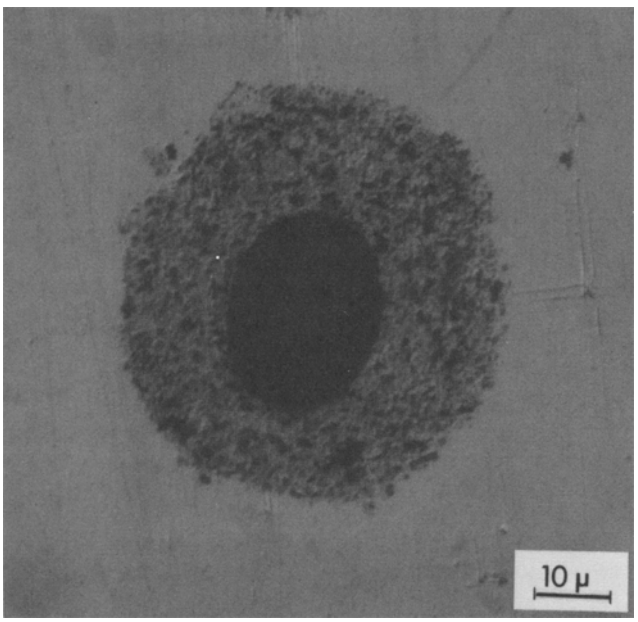


(*a*)

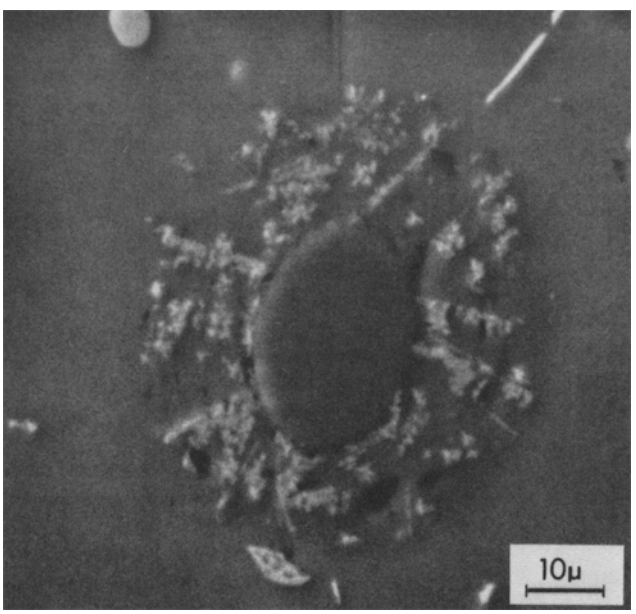


(*b*)

Fig. 9—Typical "apparent interaction zones" of $Al_2O_3$ fibers in an Al-4.5 pct Cu matrix. (*a*) Optical photomicrograph showing the presence of a multiphase material around the fiber, (*b*) back scattered electron image of the fiber in (*a*). The white areas indicate copper-rich phases; note the difference in morphology between the white particles in the interaction zone and those in the matrix, (*c*) interaction zone after heat treatment.

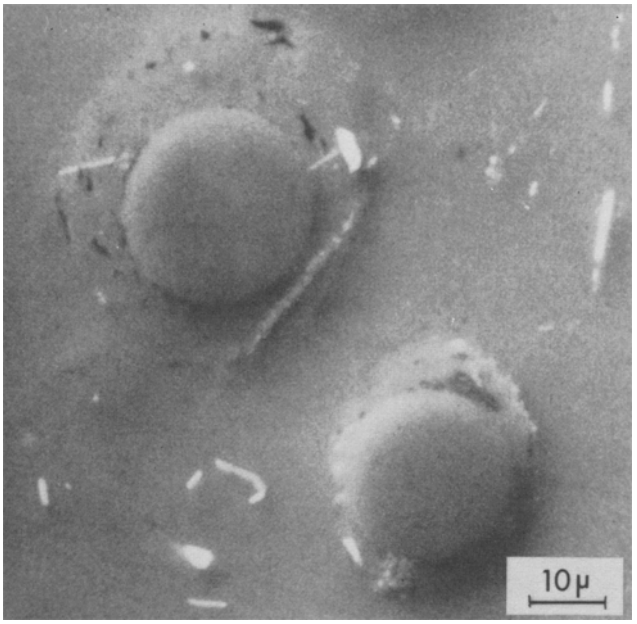


(*c*)

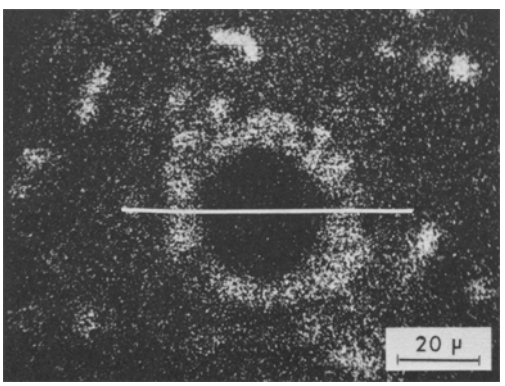


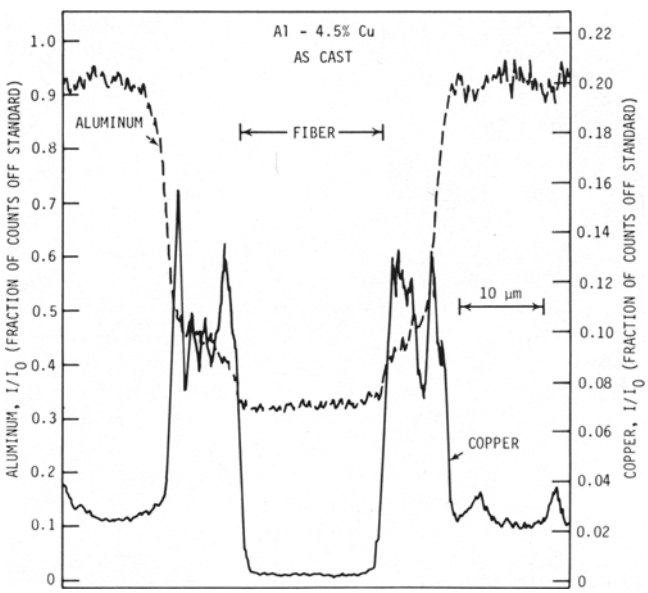


Fig. 10—Elemental Cu X-ray map and corresponding line-scanning pattern for a fiber in an Al-4.5 pct Cu matrix composite (as cast). The line on the map denotes the approximate scanning path.

zone either did not respond to the etchants used or showed a different coloration than the second phases in the matrix of the composite. Therefore, it was concluded that the Cu-rich "white phase" was different from the intermetallic compounds noted above.

Microprobe X-ray analysis was performed on samples of this composite in the as-cast and heat treated (24 h at 800 K) conditions. In the case of the former, the elemental copper map shows a distinct accumulation of this alloying element around the fiber, Fig. 10. Unlike the case of the Al-Mg alloys, the distribution is irregular due to the presence of fairly large Cu-rich clusters in the interaction zone. Several copper peaks ranging in $I/Io$ values from 0.10 to 0.20 were detected across the interaction zone of the as-cast material; however, in contrast to the Al-Mg alloys the largest peak does not necessarily occur at the fiber boundary. Examination of the sample after heat treatment revealed that the copper enrichment had disappeared and only residual copper peaks ($I/Io$ from 0.03 to 0.08) were obtained, Fig. 11. It was also noted that although the copper content in the interaction zone decreased to almost the matrix level, the aluminum content increased only to an intermediate value. Since

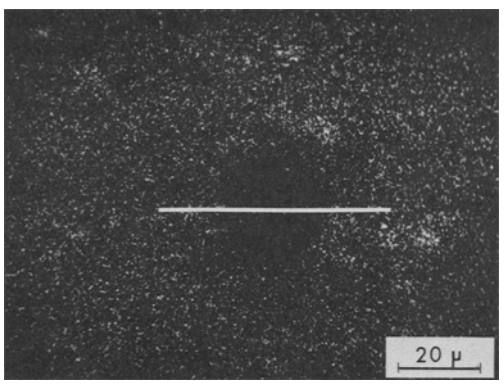


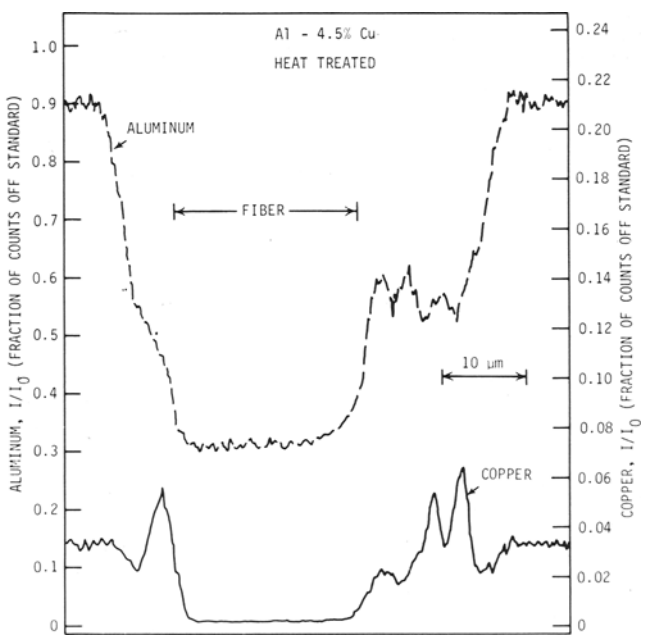


Fig. 11—Elemental Cu X-ray map and corresponding line-scanning pattern for a fiber in an Al-4.5 pct Cu matrix composite after heat treatment (24 h at 800 K). The line on the map denotes the approximate scanning path.

no major impurity in the metal could account for this phenomenon, the discrepancy was ascribed to the presence of a large amount of oxygen in this region.

BSE Images taken from the samples before and after heat treatment, Fig. 9($b$) and ($c$), show the disappearance of most of the finer "white phase" from the interaction zone. However, some second phase particles are still observed within this region and the matrix. This remaining second phase is probably composed of undissolved $CuAl_2$ and stable iron-rich compounds. In spite of the change in chemical compositions of the interaction zone, its optical appearance and size was not altered by the heat treatment, Fig. 12($a$) and ($b$). The observations discussed above indicate that compounds of the oxide type instead of intermetallics are most likely responsible for the appearance of the interaction zone.

Examination of thinned specimens in transmission electron mode again showed the existence of an intimate bond between the fibers and the surrounding material. EDS spot analysis revealed that at least two distinct phases were present at the fiber boundary. First, a significant portion of each fiber surface was in contact with a Cu-rich phase which was also observed throughout the interaction zone. The second phase, detected in limited amounts right next to some of the fiber grains and extensively throughout the interaction zone, was identified as very fine $\alpha$-$Al_2O_3$ from an electron diffraction ring-pattern.

The main hypothesis examined to explain the presence of the Cu-rich "white phase" in the interaction zone was the possible formation of a copper aluminate from any of the following reactions:

$$[Cu] + 1/2\,(O_2) + \langle Al_2O_3\rangle = \langle CuAl_2O_4\rangle \quad [5]$$

$$[Cu] + 2\,[Al] + 2\,(O_2) = \langle CuAl_2O_4\rangle \quad [6]$$

$$[Cu] + [Al] + (O_2) = \langle CuAlO_2\rangle \quad [7]$$

which have negative free energies at the processing temperature of ~910 K, see Table II.

As in the case of the magnesium spinel, some cupric aluminate could form at the expense of the $Al_2O_3$ in the fiber according to Reaction [5], or form directly in the melt and grow on the fiber surface according to Reaction [6]. In either case, this would account for the different morphology of the finer Cu-rich phase in the interaction zone and the presence of aluminum in this phase detected by EDS. Furthermore, it was calculated that $CuAl_2O_4$ is unstable at the heat treating temperature ($\Delta G_{800\ K} > 0$) and should decompose into $Al_2O_3$ and CuO. The CuO in turn may be reduced by the aluminum to metallic copper which would then diffuse into the matrix, leaving more $Al_2O_3$ behind. This is consistent with the observed migration of copper away from the fiber during the heat treatment, and the lack of change in the optical appearance of the interaction zone. Formation of the cuprous aluminate $CuAlO_2$, according to Reaction [7] is also thermodynamically possible, but this product is less stable than the $CuAl_2O_4$.[24]

The different hypotheses outlined above are not mutually exclusive, and it is possible that both oxides and metallic phases are present in the interaction zone. Since the formation of copper aluminate at the expense of $Al_2O_3$ in the fiber is feasible in the oxygen-

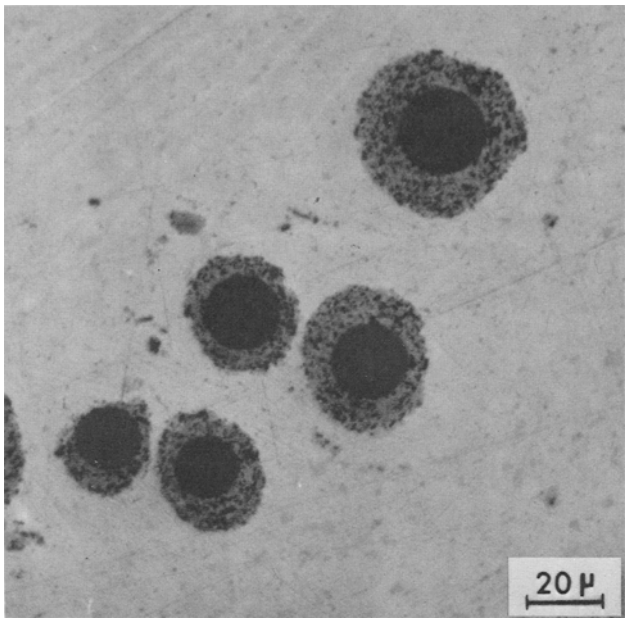


(a)

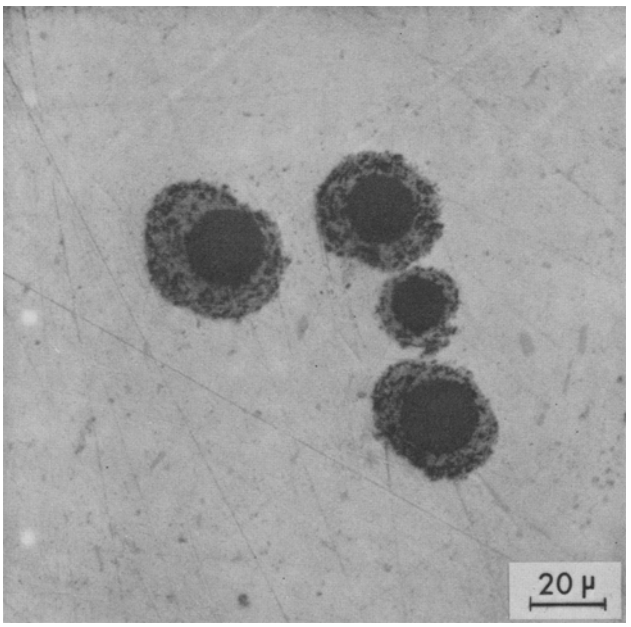


(c)

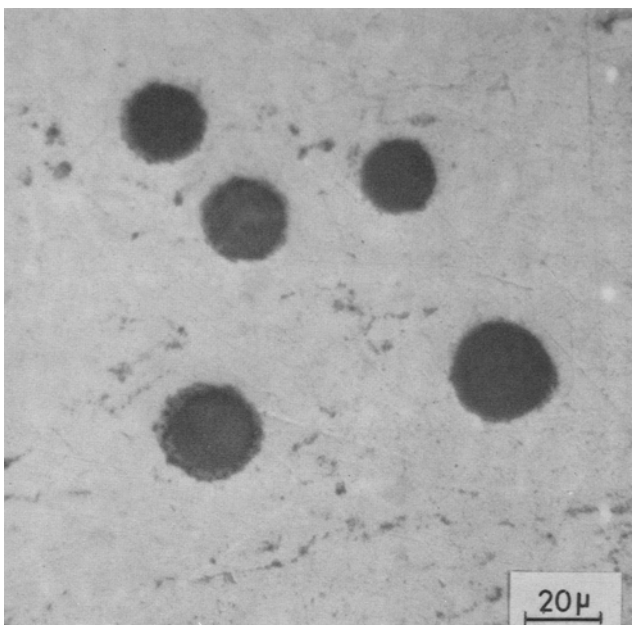


(b)

Fig. 12—Optical photomicrographs of "apparent interaction zones" in (*a*) Al-4.5 pct Cu alloy as cast, (*b*) same after 24 h at 800 K, (*c*) Al-4.5 pct Cu-0.8 pct Mg as cast.

saturated melt, this may account for the surface changes that induced wetting. However, no comprehensive explanation regarding the nature and kinetics of this mechanism is available at this time.

4. Interactions in the Al-Cu-Mg/$Al_2O_3$ System. Additions of 0.8 and 2 pct Mg to an Al-4.5 pct Cu alloy were used to study the combined effect of these two elements on the interface interactions between $Al_2O_3$ fibers and aluminum melts.

The main effect of the magnesium was to significantly reduce the extent of interaction observed in the Al-Cu specimens. This is evident from the photomicrographs of Fig. 12(*a*) and (*c*), where the addition of 0.8 pct Mg has suppressed most of the thick "apparent interaction zone" which was characteristic of the Al-4.5 pct Cu matrix composite. It should be mentioned that the residence time of the fibers in the Al-Cu-Mg melt was much longer than that in the binary alloy (Runs No. 1 and No. 2 in Table I). Furthermore, the general trend for the development of the interaction zone as a function of time in the Al-4.5 pct Cu-2 pct Mg alloy was different from the equivalent binary Al-4.5 pct Cu and Al-2 pct Mg matrices as illustrated in Fig. 6.

Elemental X-ray maps for Mg and Cu again showed preferential accumulation of these elements at the fiber boundary, Fig. 13. Even though the specimen in this figure contained 0.8 pct Mg, peaks with $I/Io$ values above 0.10 were detected in the immediate vicinity of the fiber. As in the case of the individual additions, the Mg-rich zone detected by X-ray appeared continuous while the copper map revealed a more localized concentration of this element. Examination of heat treated (24 h at 800 K) specimens of the ternary alloy composite by microprobe X-ray analysis and BSEI, Figs. 13 and 14, showed an important difference between this alloy and the binary Al-4.5 pct Cu alloy. While most of the nonequilibrium second phases (*i.e.*, $CuAl_2$ and $CuMgAl_2$) of the matrix dissolved during the heat treatment, a thin Cu-rich ring was left around the fiber. This observation was further verified by microprobe scan of this region. The remaining second phases in the matrix of Fig. 14 are probably iron rich compounds or undissolved nonequilibrium second phases.

Thermodynamic analysis of the possible interactions in the ternary alloys was attempted by assuming that the activities of copper and magnesium in aluminum are not affected by the presence of each other. The results indicate that the formation of $CuAl_2O_4$ and/or CuO will be hindered by the addition of Mg which would preferentially react with $O_2$ to form $MgAl_2O_4$ and/or MgO. Furthermore, the lower processing

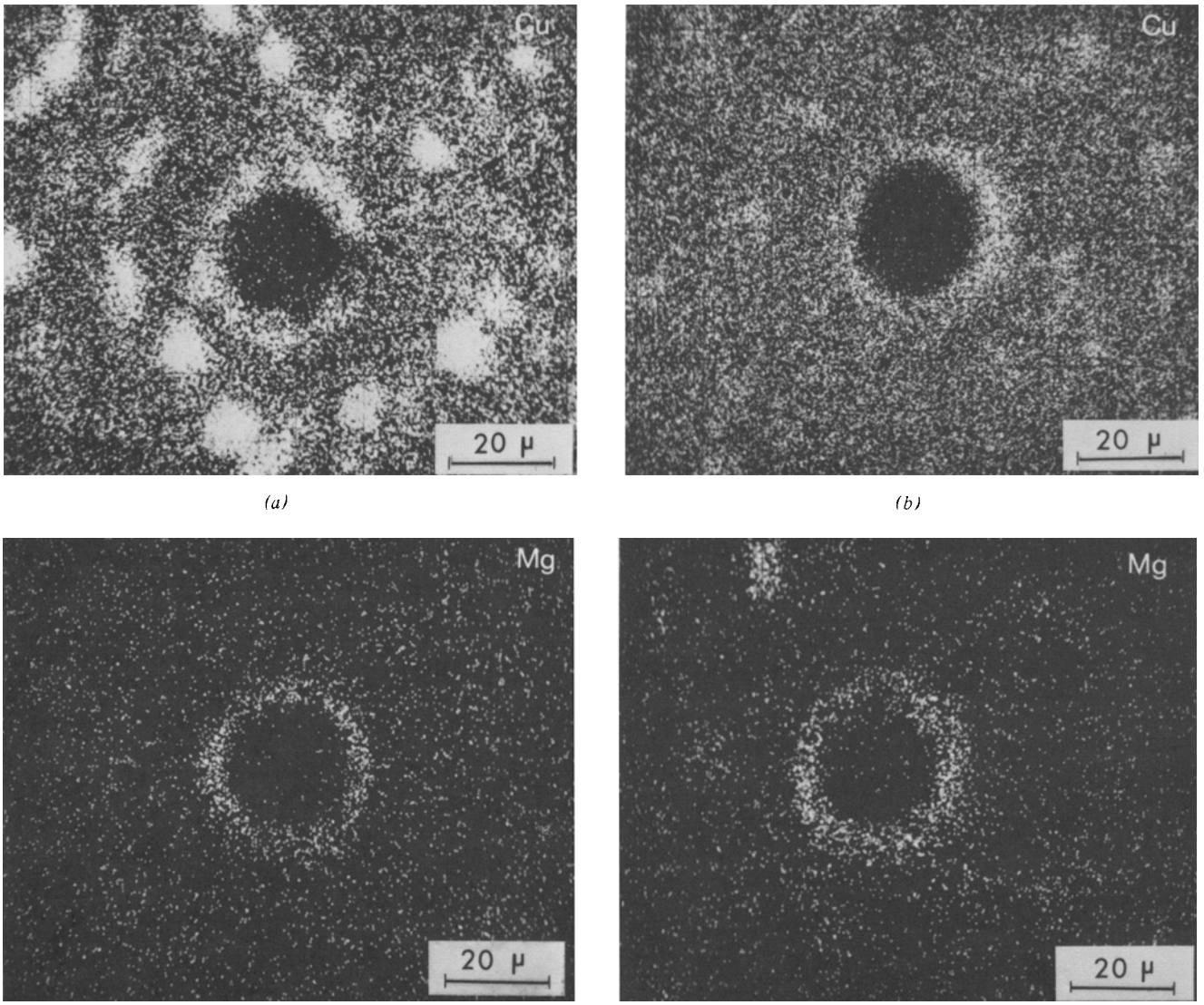


Fig. 13—Elemental Cu and Mg X-ray maps showing the effect of heat treatment on the relative distribution of alloying elements around fibers in an Al-4.5 pct Cu-0.8 pct Mg matrix composite; (*a*) and (*c*) Cu and Mg respectively, before heat treatment, (*b*) and (*d*) Cu and Mg respectively, after heat treatment.

temperature used in the case of the ternary alloys is expected to have a pronounced effect on the driving force for the formation of copper aluminate, which becomes nil at ~885 K, see Table II. The smaller amount of copper rich phase observed around the fibers in the Al-Cu-Mg alloys could thus be explained.

On the other hand, $CuAl_2O_4$ is expected to become unstable at the heat treating temperature and should decompose into $Al_2O_3$ and CuO. However, when magnesium is present the more stable $MgAl_2O_4$ product could form around the existing $CuAl_2O_4$ particles, thereby creating a barrier for the outward diffusion of copper. This hypothesis and the possible effect of magnesium on the diffusion coefficient of copper, especially in the magnesium-enriched zone around the fibers, could account for the slower homogenization kinetics of copper observed in the ternary system.

5. Mechanical Behavior of the Interfaces. The desirability of an oxide or spinel bond in $Al_2O_3$-metal matrix composites has been pointed out by several investigators, as discussed earlier. Microexamination of the interaction zones in aluminum alloy–$Al_2O_3$ fiber composites produced in the partially-solid state indicated that compounds of the oxide type were present at the fiber boundary. Examples of the fracture surfaces of tensile specimens of an Al-2 pct Mg/12 vol pct fiber and an Al-4.5 pct Cu-2 pct Mg/14 vol pct fiber composite are shown in Fig. 15. The general findings from examination of the fractured surfaces are summarized below:

a) no major differences were observed between the heat treated and as-extruded specimens of the same composite;

b) some fiber "pull-out" occurred in all the samples, but the failure appeared to be through the metal and not the interface, as indicated by the conical cavities with the rippled surfaces in Figs. 15(*a*) and (*b*);

c) apparently more "pull-out" occurred in the Al-2 pct Mg matrix composite, as expected from the lower strength of the matrix;

d) in some places, where the fiber ends were ex-

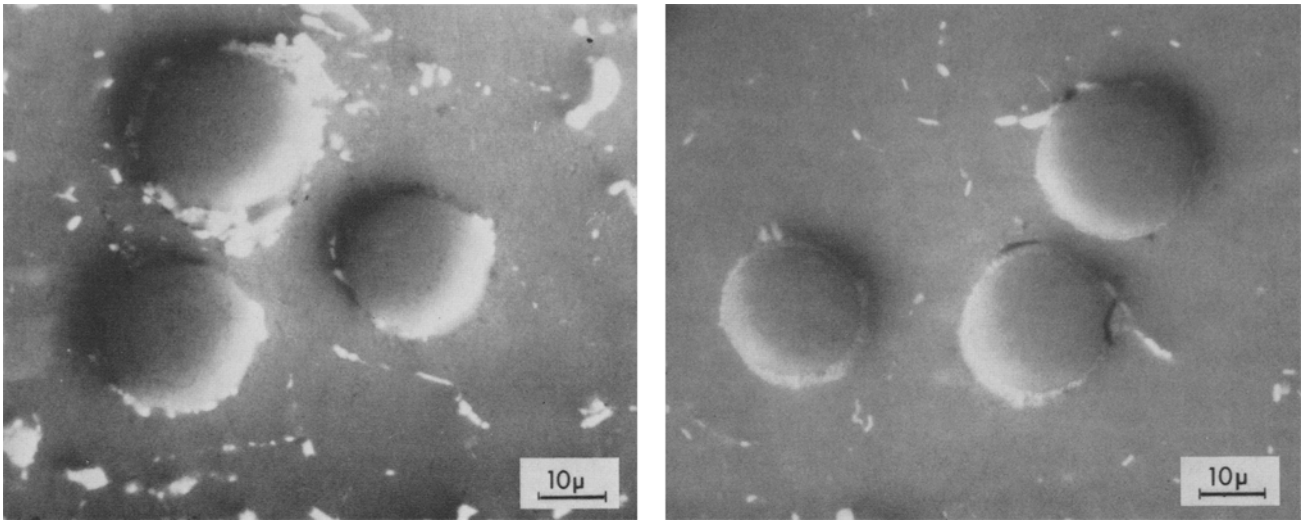


(a) (b)

Fig. 14—B.S.E. images of fibers and their surroundings in an Al-4.5 pct Cu-0.8 pct Mg; (*a*) before heat treatment, (*b*) after 24 h at 800 K. *Note the disappearance of the matrix second phase but the retention of a finer Cu rich phase around the fibers after treatment.*

posed at the surface, it appears that the matrix sheared away from the fiber ends, leaving metal adherences; an example of this is shown in Fig. 15(*d*).

These composites had interaction zones in the range of 1 $\mu$m or less and not the thick layers discussed in the previous sections. Since in most cases the failure seems to occur through-the-matrix, it is concluded that under the present conditions (tensile strengths of 200 to 380 MPa) the interfaces were strong enough to permit the transfer of loads. However, the effect of the short length ($l/d \sim 15$) and misalignment of the fibers did not permit a true estimation of the bond strength.

## IV. CONCLUSIONS

1) Homogeneous dispersions of $Al_2O_3$ fibers were obtained by adding them to agitated, partially-solid slurries of Al-Mg, Al-Cu and Al-Cu-Mg alloys. The fibers appeared wetted and bonded to the matrix in the final composite product. It is postulated that the fibers added to the metal slurries were kept dispersed by the agitation and the moving primary solid particles until they developed some sort of interaction with the matrix. Incorporation and wetting were thus readily achieved even in alloy systems that normally exhibit a nonwetting behavior.

2) Attempts to incorporate the fibers into static

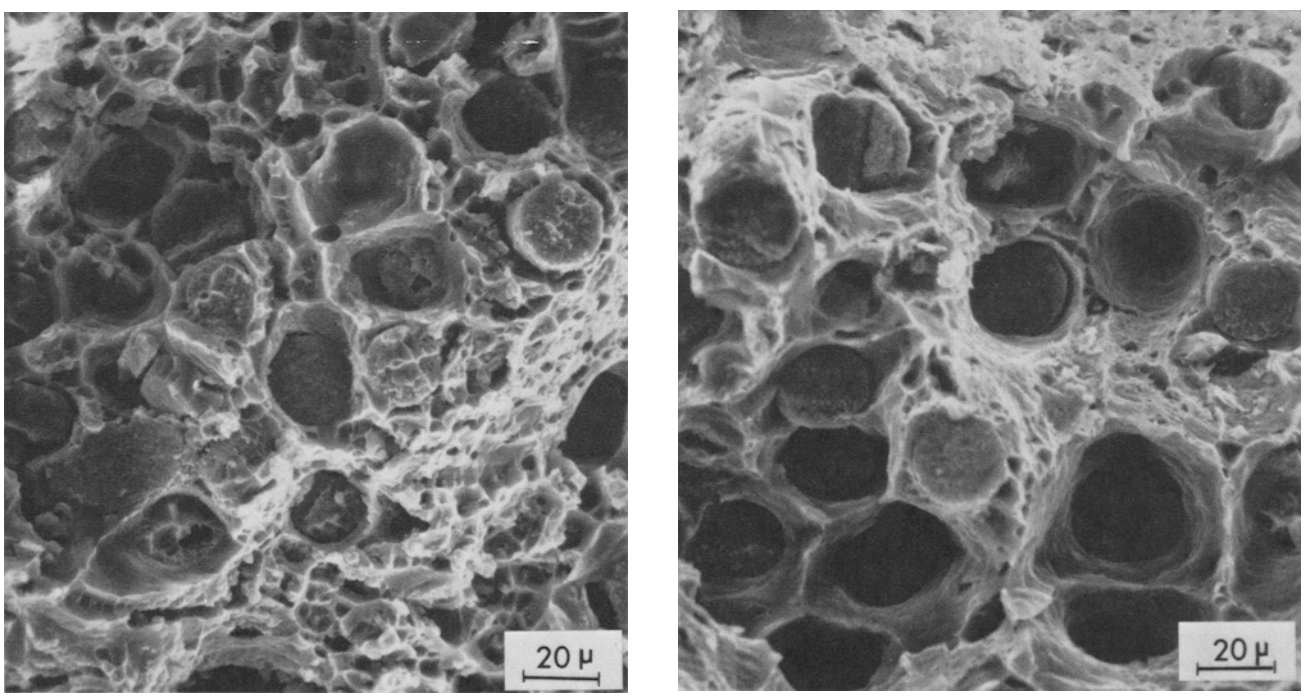


(a) (b)

Fig. 15—SEM views of fracture surfaces in Al-matrix composites. (*a*) Al-4.5 pct Cu-2 pct Mg/14 vol pct fiber, (*b*), (*c*), and (*d*) Al-2 pct Mg/12 vol pct fiber.

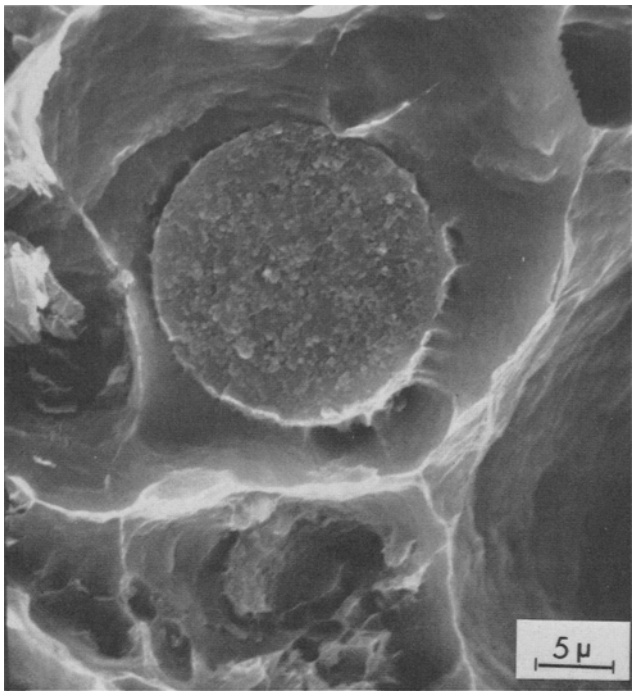


(c)

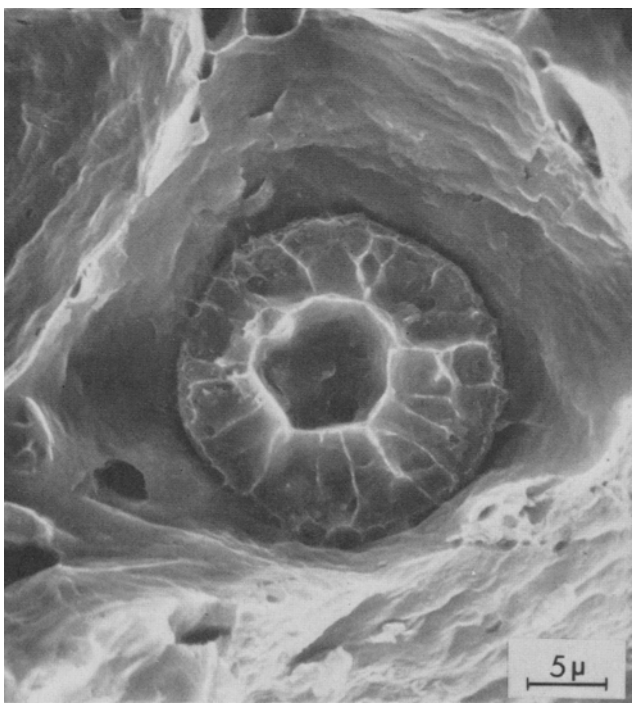


(d)

Fig. 15—Continued.

baths of the alloys above their liquidus temperatures were unsuccessful.

3) Microscopic examination of the composites prepared revealed the existence of a significantly altered microstructure around the $Al_2O_3$ fibers which consists of a fine multiphase material. Features common to all the structures were the existence of an intimate bond, the absence of voids at the fiber boundary and the presence of fine polycrystalline $\alpha$-$Al_2O_3$ in the interaction zone. The average maximum thickness of this "apparent interaction zone" depends on residence time and alloy composition. No changes in the dimensions and optical appearance of the interaction zone were observed after heat treatment of the composites.

4) Interactions between $Al_2O_3$ fibers and Al-Mg alloys resulted in the formation of a Mg-rich region around the fibers which was retained during heat treatment. This is attributed to the presence of $MgAl_2O_4$ and MgO at the fiber boundary in addition to $\alpha$-$Al_2O_3$. Changes in appearance of the interaction zone were observed for different magnesium contents in the alloy.

5) Interactions in the Al-Cu system produced a distinctive accumulation of copper around the fibers. The copper occurs in the form of discrete particles of a Cu-rich phase which disappears with heat treatment. It is suggested that $CuAl_2O_4$ may be present along with $\alpha$-$Al_2O_3$ and possibly $CuAl_2$ in the interaction zone.

6) Addition of small amounts of magnesium to the Al-Cu alloy significantly reduced the extent of interaction observed. Both magnesium and copper enrichments around the fiber were detected in this case, but as opposed to the Al-Cu matrix, the Cu-rich phase was still present at the fiber boundary after heat treatment. Experimental observations indicate that $MgAl_2O_4$, $\alpha$-$Al_2O_3$ and possibly $CuAl_2O_4$ coexist in the interaction zone.

7) The results of this study suggest that a compound of the aluminate type may form on the fiber surface and provide the required bond with the surroundings. This reaction will be enhanced in the presence of oxygen which is introduced by the vigorous agitation during the fabrication step.

8) Examination of fracture surfaces of the composites revealed that in general the failure was not at the interface but rather by plastic flow of the matrix around the fibers.

## ACKNOWLEDGMENTS

This project was sponsored by The Army Research Office in Research Triangle Park, North Carolina under contract DAAG-29-76-G-0170. Technical monitor of the project was Dr. John C. Hurt. Special thanks are due to Dr. Aldo M. Reti of Handy and Harman, Fairfield, Connecticut for the extrusion of the composites, and Drs. H. Hartman and A. K. Dhingra of E. I. Dupont Experimental Station for their help in the procurement of the $Al_2O_3$ FP fiber. Technical contributions to the microstructural analysis from Mr. Ian Ward and Mr. John Woodhouse of the Materials Research Laboratory, University of Illinois, are gratefully acknowledged.

## REFERENCES

1. L. J. Ebert and P. Kennard-Wright: *Composite Materials*, 1st ed., vol. 1, p. 31, Academic Press, New York, 1974.
2. A. G. Metcalfe and M. J. Klein: *Ibid.*, p. 125.
3. W. H. Sutton: *Whisker Technology*, 1st ed., p. 273, Wiley Interscience, N. Y., 1970.
4. A. P. Levitt: *Ibid.*, p. 245.
5. R. L. Mehan: *Metal Matrix Composites*, p. 29, STP 438, ASTM, 1968.
6. M. J. Moore, E. Feingold and W. H. Sutton: *Interfaces in Composites*, p. 90, STP 452, ASTM, Philadelphia, Penn., 1969.
7. R. L. Mehan: *J. Compos. Mater.*, 1970, vol. 4, p. 90.
8. A. K. Dhingra and W. H. Krueger: *Fiber FP, Continuous Alumina Yarn*, Report by E. I. Dupont de Nemours and Co., Inc., Wilmington, Del., 1974.
9. K. M. Prewo: Report R77-912 245-3, Contract N00014-76-C-0035, United

Technologies, East Hartford, Conn., May, 1977.
10. D. T. Livey and P. Murray: *Plansee Proc., 2nd Seminar, (Reutte, Tyrol, 1955),* pp. 375-404, 1956.
11. R. D. Carnahan, T. L. Johnson and C. H. Li: *J. Amer. Ceram. Soc.,* 1958, vol. 41, pp. 343-47.
12. K. Prabriputaloong and M. R. Piggott: *Surface Sci.,* 1974, vol. 44, pp. 585-97.
13. M. Nicholas: *J. Mater. Sci.,* 1968, vol. 3, pp. 571-76.
14. S. M. Wolf, A. P. Levitt and J. Brown: *Chem. Eng. Progr.,* 1966, vol. 62, pp. 74-78.
15. J. A. Champion, B. J. Keene and J. M. Sillwood: *J. Mater. Sci.,* 1969, vol. 4, pp. 39-49.
16. J. Brennan and J. A. Pask: *J. Amer. Ceram. Soc.,* 1968, vol. 51, pp. 569-73.
17. R. E. Tressler: *Composite Materials,* 1st ed., vol. 1, p. 285, Academic Press, New York, 1974.
18. W. A. Weyl: Proc. No. 46, p. 506, ASTM, 1946.
19. G. Katz: *Thin Solid Films,* 1976, vol. 33, pp. 99-105.
20. J. G. Lindsay, W. T. Bakker and E. W. Dewig: *J. Amer. Ceram. Soc.,* 1964, vol. 47, pp. 90-94.
21. J. J. Comer, N. C. Tombs and J. F. Fitzgerald: *J. Amer. Ceram. Soc.,* 1966, vol. 49, pp. 237-40.
22. M. W. Shumate: *Interactions of Molten Aluminum with Phosphate Bonded $Al_2O_3$ Refractories* M. S. Thesis, University of Illinois, Urbana, Ill., 1977.
23. A. Sato and R. Mehrabian: *Met. Trans. B,* 1976, vol. 7B, pp. 443-51.
24. K. T. Jacob and C. B. Alcock: *J. Amer. Ceram. Soc.,* 1975, vol. 58, pp. 192-95.
25. O. Kubaschewski, E. Ll. Evans and C. B. Alcock: *Metallurgical Thermochemistry,* 4th ed., Pergamon Press, New York, 1967.
26. R. Hultgren, P. D. Desai, D. T. Hawkins, M. Gleiser, and K. K. Kelley: *Selected Values of the Thermodynamic Properties of Binary Alloys,* ASM, Metals Park, Ohio, 1973.